

ECINADS-D6.2: A dynamic variational multiscale LES model for the simulation of bluff body flows on unstructured grids

Carine Moussaed^a, Anca Belme^c, Stephen Wornom^b, Bruno Koobus^a, Alain Dervieux^c

^a*Département de Mathématiques, Université Montpellier 2,
Place Eugène Bataillon, 34095 Montpellier cedex, France*

^b*LEMMA, 2000 Route des Lucioles, 06902 Sophia-Antipolis, France*

^c*INRIA, 2004 Route des Lucioles, 06902 Sophia-Antipolis, France*

Abstract

A variational multiscale large-eddy simulation (VMS-LES) model with dynamic subgrid scale (SGS) models is used for the prediction of flows around bluff bodies in subcritical regime. The test-cases considered in this paper consist in a circular cylinder at Reynolds number 20000, and a sphere at Reynolds numbers 10000 and 50000. A mixed finite-element/finite-volume discretization on unstructured grids is used. The separation between the largest and the smallest resolved scales is obtained through a variational projection operator and a finite-volume cell agglomeration. The dynamic version of Smagorinsky and WALE SGS models are used to account for the effects of the unresolved scales; in the VMS approach, it is only added to the smallest resolved scales. The capability of this methodology to accurately predict the aerodynamic forces acting on the cylinder and the sphere are evaluated for the different Reynolds numbers considered.

1 Introduction

In spite of an extensive research for more than a century applied to the flows in turbulent regime, their modelling remains a big challenge even today. It is commonly accepted that the physics of the flow of a continuous fluid is well represented by the Navier-Stokes equations. Three main axes of simulation appear : the direct numerical simulation, the large eddy simulation and the statistical modelisation. The direct numerical simulation (DNS) numerically resolves all the significant scales of motion in a flow down to the Kolmogorov scales, corresponding to the scales responsible for the dissipation of energy in the flow. To achieve this, Blazek (2001) [11] pointed out that a sufficient spatial resolution and CPU time requirement for DNS is proportional to $Re^{\frac{3}{4}}$ and Re^3 respectively (Re=Reynolds number). This agrees with the investigation of Frolich et al. (1998) [15] in determining the required resolution for DNS. Thus, it is still not practical to accurately resolve the non-linear nature and three dimensional characteristics of turbulence at rather moderate and high Reynolds numbers using DNS with the currently available computer technology. In an attempt to resolve flow at higher Reynolds number of 10,000 using DNS, Tremblay concluded that the simulation needs about 80 computing days running on a 32 processor parallel computer system. This could mean that DNS is still not practical for engineering applications and for the time being, applications are restricted to lower Reynolds number. The statistical simulation consist in time-averaging the Navier-Stokes equations. The latter are usually referred as the Reynolds Averaged Navier Stokes (RANS) models, where the unsteadiness of the flow is averaged out. In the RANS model, all aspects of turbulence are modelled. Large eddy simulation (LES) is classified as a space filtering method in CFD. LES directly computes the large-scale turbulent structures which are responsible for the transfer of energy and momentum in a flow while modelling the smaller scale of dissipative and more isotropic structures. In order to distinguish between the large scales and small scales, a filter function is used in LES. A filter function dictates which eddies are large by introducing a length scale, the characteristic filter width of the simulation. All eddies larger than this length scale are resolved directly, while those smaller than the length scale are approximated. Today large-eddy simulations (LES) are increasingly used for engineering and industrial applications, at least for those flows for which the RANS approach

encounters difficulties in giving accurate predictions. Paradigmatic examples of such flows are bluff-body wakes. A RANS calculation is little dependent on the number of Reynolds and little greedy in CPU time, but provides only a limited information: average and statistical fields in a point of the turbulence only. However the RANS model presents a strong degree of empiricism, making them little reliable in certain types of flow. LES is the midway between DNS and RANS modelisation as regards informations acquired on flow and the cost of calculating. A variational multiscale (VMS) approach has been proposed in [22]. This approach might be effective in obtaining a good compromise between accuracy and computational requirements. The main idea of VMS-LES is to decompose, through Galerkin projection, the resolved scales into the largest and smallest ones and to add the SGS model only to the smallest ones. This is aimed at reducing the excessive dissipation introduced by eddy-viscosity SGS models also on the large scales.

The present work is part of a research activity aimed at investigating the contribution of the dynamic procedure used with the classical LES and especially with the Variational Multiscale (VMS) LES approach, used together with an industrial numerical set-up. This industrial numerical set-up is based on a mixed finite-volume/finite-element discretization on unstructured grids, second order accurate in space and time. The VMS approach is particularly attractive for variational numerical methods and unstructured grids, because it is easily incorporated in such formulations [23, 4] and the additional computational costs with respect to classical LES are very low, while other approaches may bring rather large additional complexity and computational costs [20]. The used VMS approach is the one proposed in [4], in which the projection operator in the largest resolved scale space is defined through finite-volume cell agglomeration. Two different eddy-viscosity SGS models are considered, both for classical LES and VMS-LES, viz. the dynamic version [28, 29] of Smagorinsky [24] and Wall-Adapting local Eddy-Viscosity (WALE) models [26]. We propose to use for numerics a second-order accurate MUSCL upwind scheme equipped with a tunable dissipation made of sixth-order [1] spatial derivatives of all flow variables. The classical LES and VMS methodology have been applied [8], together with different eddy-viscosity SGS models, to the flow around a circular cylinder at a Reynolds number 20000, and around a sphere at Reynolds numbers 20000 and 50000. Results for the considered circular cylinder test-case are reported in [19, 12]. For the case of the sphere, see [7] for Reynolds number 10000 and [13, 17] for 50000. The main aim of the present work is to investigate whether the VMS-LES approach with dynamic SGS models is able to predict, on an unstructured grid as those often used in industrial applications, the variation of aerodynamic forces acting on the considered bluff bodies and to capture the important flow features for such problems.

2 Methodology

2.1 Classical LES approach

Large eddy simulation (LES) is classified as a space filtering method in CFD, in order to get rid of the high frequency fluctuations. It consists in filtering in space the Navier-Stokes equations. In order to separate the large scales and small scales, a filter function is used in LES. All eddies larger than the filter are resolved directly, while those smaller than the filter are approximated. In LES, each variable W of the flow is separated into a filtered, resolved part \bar{W} and a sub-filter, unresolved part, w' .

$$W = \bar{W} + w' \quad (1)$$

The filtered Navier-Stokes equations for compressible flows and in conservative form are considered. In fluid flow around an immersed object, shear stress occurs because not all the fluid exerts forces tangentially to the wall of the object. This results in the appearance of the stress terms in the equations governing fluid flow. After dividing the Navier-Stokes Equation into filtered and sub-filter components, unknown stress terms arise due to the nonlinearity of the equations and the shear stress of the flow. These terms need to be approximated to solve the filtered Navier-Stokes Equations. In modeling the SGS terms resulting from filtering the Navier-Stokes equations, the effects of compressibility present in the SGS fluctuations are assumed low and the heat transfer and temperature gradients are assumed moderate. Thus, the retained SGS term in the momentum equations is the classical SGS stress tensor:

$$M_{ij} = \overline{\rho u_i u_j} - \overline{\rho} \tilde{u}_i \tilde{u}_j \quad , \quad (2)$$

where the over-line denotes the grid filter and the tilde the density-weighted Favre filter ($\tilde{f} = (\overline{\rho f}) / (\overline{\rho})$). The isotropic part of M_{ij} can be neglected under the assumption of low compressibility effects in the SGS fluctuations [35]. The deviatoric part, T_{ij} , is expressed by an eddy viscosity term:

$$T_{ij} = -2\mu_{\text{sgs}} \left(\widetilde{S}_{ij} - \frac{1}{3} \widetilde{S}_{kk} \right) \quad , \quad (3)$$

where \widetilde{S}_{ij} being the resolved strain tensor $\widetilde{S}_{ij} = \frac{1}{2} \left(\frac{\partial u_i}{\partial x_j} + \frac{\partial u_j}{\partial x_i} \right)$ and μ_{SGS} the SGS viscosity.

In the total energy equation, the effect of the SGS fluctuations has been modeled by the introduction of a constant SGS Prandtl number to be a priori assigned:

$$Pr_{\text{sgs}} = C_p \frac{\mu_{\text{sgs}}}{K_{\text{sgs}}} \quad (4)$$

where K_{sgs} is the SGS conductivity coefficient; it takes into account the diffusion of total energy caused by the SGS fluctuations and is added to the molecular conductivity coefficient. We refer to [5] and [20] for a more detailed discussion of the simplifying assumptions leading to the adopted SGS modeling.

2.2 Variational Multiscale LES approach

The VMS formulation consist in splitting between the large resolved scales (LRS) i.e. those resolved on a virtual coarser grid, and the small resolved ones (SRS). The VMS-LES method does not compute the SGS component of the solution, but modelizes its effect on the small resolved scales which corresponds to the highest level of discretization, and preserves the Navier-Stokes model for the large resolved scales. In the present work, we adopt the VMS approach proposed by Koobus and Farhat [4] for the simulation of compressible turbulent flows through a finite volume/finite element discretization on unstructured tetrahedral grids. Let V_{FV} be the space spanned by Φ_k , the finite volume basis function and V_{FE} the one spanned by ψ_k , the finite element basis function. In order to separate coarse- and fine- scales, these spaces are decomposed as: $\psi_k = \overline{\psi}_k + \psi'_k$ and $\phi_k = \overline{\phi}_k + \phi'_k$ where overline denotes a coarse scale and the prime a fine scale. Consequently to this decomposition, the variables of the flow are decomposed as follows:

$$W = \overline{W} + W' + W^{SGS} \quad (5)$$

where \overline{W} are the LRS, W' the SRS and W^{SGS} are the unresolved scales. In [4], a projector operator based on spatial average on macro-celles is defined in the LRS space to determinate the basis functions of the LRS space:

$$\overline{\psi}_k = \frac{Vol(C_k)}{\sum_{j \in I_k} Vol(C_j)} \sum_{j \in I_k} \psi_j \quad (6)$$

for finite volumes, and

$$\overline{\phi}_k = \frac{Vol(C_k)}{\sum_{j \in I_k} Vol(C_j)} \sum_{j \in I_k} \phi_j \quad (7)$$

for finite elements. $Vol(C_j)$ designate the volume of C_j , the cell around the vertex j . $I_k = \{j/C_j \in C_{m(k)}\}$ and $C_{m(k)}$ denotes the macro-cell containing the cell C_k . The macro-celles are obtained by a process known as agglomeration [2]. The SGS model which modelizes the dissipatif effect of the unresolved scales on the resolved scales is only added to the fine-resolved scales. The term bellow is added to the fine-scale momentum equation

$$\int_{\Omega} \tau' \nabla \Phi' \, d\Omega \quad (8)$$

Where $\tau'_{ij} = -\mu'_t (2S'_{ij} - \frac{2}{3} S'_{kk} \delta_{ij})$ and $S'_{ij} = \frac{1}{2} \left(\frac{\partial u'_i}{\partial x_j} + \frac{\partial u'_j}{\partial x_i} \right)$ and μ'_t designate the viscosity of the SGS model used to close the problem. Likewise, the term

$$\int_{\Omega} \frac{C_p \mu'_t}{Pr_{sgs}} \nabla T' \cdot \nabla \Phi' d\Omega \quad (9)$$

is added to the fine scales energy equation. C_p is the specific heat at constant pressure and Pr_t is the subgrid-scale Prandtl number which is assumed to be constant.

2.3 SGS models

Smagorinsky

To approximate the SGS Reynolds stress a SGS model can be employed. The most commonly used SGS models in LES is the Smagorinsky model in which the eddy viscosity is defined by

$$\mu_{sgs} = \bar{\rho} (C_s \Delta)^2 \left| \widetilde{S} \right|, \quad (10)$$

where Δ is the filter width, C_s is the Smagorinsky coefficient and $\left| \widetilde{S} \right| = \sqrt{2 \widetilde{S}_{ij}^2}$. A typical value for the Smagorinsky coefficient is $C_s = 0,1$ that is often used, especially in the presence of the mean shear.

WALE

The second SGS model we considered is the Wall-Adapting Local Eddy -Viscosity (WALE) SGS model proposed by Nicoud and Ducros [26]. The eddy-viscosity term μ_{sgs} of the model is defined by:

$$\mu_{sgs} = \bar{\rho} (C_w \Delta)^2 \frac{(\widetilde{S}_{ij}^d \widetilde{S}_{ij}^d)^{\frac{3}{2}}}{(\widetilde{S}_{ij} \widetilde{S}_{ij})^{\frac{5}{2}} + (\widetilde{S}_{ij}^d \widetilde{S}_{ij}^d)^{\frac{5}{4}}} \quad (11)$$

with being the symmetric part of the tensor $g_{ij}^2 = g_{ik} g_{kj}$, where $g_{ij} = \partial \tilde{u}_i / \partial x_j$:

$$\widetilde{S}_{ij}^d = \frac{1}{2} (g_{ij}^2 + g_{ji}^2) - \frac{1}{3} \delta_{ij} g_{kk}^2$$

Dynamic model

Historically, the constant (C_s, C_w) appearing in the expression of the viscosity of a SGS model was often arbitrarily set to a constant over entire flow field. For general inhomogeneous flows, it can be a strong function of space. This constant is replaced, according to Germano et al. [28], with a dimensionless parameter $C(x, t)$ that is allowed to be a function of space and time. This dynamic procedure provides a systematic way of adjusting C_s or C_w allowing it to be a function of position which is desirable for inhomogeneous flows. A novel feature of this method is that $C(x, t)$ is estimated dynamically using information from the resolved scales making the model self-tuning. The so-called dynamic model [28] has been refined [30, 29] over the past several years and has been successfully used to study a variety of complex inhomogeneous flows. The first step in the dynamic model consists in the introduction of a second filter, larger than the filter width, which is called the test-filter. The test-filter is applied to the grid filtered Navier Stokes equations, then, the sub test-scale stress is defined as

$$M_{ij}^{test} = \widehat{\rho \mathbf{u}_i \mathbf{u}_j} - (\hat{\rho})^{-1} \left(\widehat{\rho \mathbf{u}_i} \widehat{\rho \mathbf{u}_j} \right) \quad (12)$$

and, can be written using a Smagorinsky or WALE model, as

$$M_{ij}^{test} - \frac{1}{3} M_{kk}^{test} \delta_{ij} = -C \hat{\Delta}^2 \hat{\rho} g(\hat{\mathbf{u}}) \hat{P}_{ij} \quad (C \text{ denotes } C_w^2 \text{ or } C_s^2) \quad (13)$$

We recall that the over-line denotes the grid filter, the tilde the Favre filter and the chapeau the test-filter, and C , as originally shown by Germano et al. [28], is chosen so that the subgrid-scale is consistent with the subtest-scale. The quantity

$$\mathcal{L}_{ij} = M_{ij}^{test} - \hat{M}_{ij} = \widehat{\rho \tilde{\mathbf{u}}_i \tilde{\mathbf{u}}_j} - (\hat{\rho})^{-1} \left(\widehat{\rho \tilde{\mathbf{u}}_i} \widehat{\rho \tilde{\mathbf{u}}_j} \right) \quad (14)$$

is called the Leonard stress. In order to determine the constant, one can compare L_{ij} to the value that would be obtained using the SGS model (Smagorinsky or WALE). This leads to

$$L_{ij} = \mathcal{L}_{ij} - \frac{1}{3} \mathcal{L}_{kk} \delta_{ij} = (C \Delta^2) B_{ij} \quad (15)$$

where

$$B_{ij} = \widehat{\bar{\rho}g(\hat{\mathbf{u}})\hat{P}_{ij}} - \left(\frac{\hat{\Delta}}{\Delta}\right)^2 \hat{\rho}g(\hat{\mathbf{u}})\hat{P}_{ij}$$

Equation (15) represents six equations with one unknown. The unknown $(C\Delta^2)$ has to satisfy

$$L_{ij} = (C\Delta^2)B_{ij} \quad (16)$$

This system of six equations can be resolved using the least squares approach. $(C\Delta^2)$ minimizes the quantity

$$Q = (L_{ij} - (C\Delta^2)B_{ij})^2 \quad (17)$$

Thus, $(C\Delta^2)$ is found by setting $\frac{\partial Q}{\partial (C\Delta^2)} = 0$, from which we derive the value of $(C\Delta^2)$:

$$(C\Delta^2) = \frac{L_{ij}B_{ij}}{B_{pq}B_{pq}} . \quad (18)$$

A drawback to the development of any dynamic version based on the Germano-identity [28] could be caused by the sensitivity of SGS models having the correct behavior near the wall to the filtering procedure and the stabilization method. A simple way to avoid this inconvenient is to have a sensor able to detect the presence of the wall, without a priori knowledge of the geometry, so that the considered SGS model of WALE adapts the classical constant of the model, which is equal to 0,5 in the near wall region, and compute the constant dynamically otherwise. We adapt the sensor proposed by Toda and Truffin in [Nicoud SVS], the expression of which is:

$$SVS = \frac{S_{ij}^d S_{ij}^{d\frac{3}{2}}}{S_{ij}^d S_{ij}^{d\frac{3}{2}} + S_{ij} S_{ij}^3} \quad (19)$$

This parameter has the property to behave like y^{+3} , to be equal to 0 for pure shear flows and 1 for pure rotating flows.

3 Numerical discretization

The choice of the numerical discretization will influence in two ways this study. First, we use a numerical scheme for compressible flow which needs to be stabilized by numerical dissipation. As discussed in the Introduction, it is compulsory that the numerical dissipation does not interfere with the LES model. A particular attention is paid to this issue. Second, the VMS formulation is based on the basis functions of the scheme. This issue is addressed in the next section. We recall now the main features of the numerical scheme. Further details can be found in [1] and in [3].

The governing equations are discretized in space using a mixed finite-volume/finite-element method applied to unstructured tetrahedrizations. The adopted scheme is vertex centered, i.e. all degrees of freedom are located at the vertices. P1 Galerkin finite elements are used to discretize the diffusive terms.

A dual finite-volume grid is obtained by building a cell C_i around each vertex i ; the finite-volume cells are built by the rule of medians: the boundaries between cells are made of triangular interface facets. Each of these facets has a mid-edge, a facet centroid, and a tetrahedron centroid as vertices. The convective fluxes are discretized on this tessellation by a finite-volume approach, i.e. in terms of the fluxes through the common boundaries between each couple of neighboring cells:

$$\sum_{j \in V(i)} \int_{\partial C_{ij}} \mathcal{F}(W, \vec{n}) d\sigma , \quad (20)$$

where $V(i)$ is the set of neighboring nodes to vertex i , ∂C_{ij} is the boundary between cells C_i and C_j , and \vec{n} is the outer normal to the cell C_i and $\mathcal{F}(W, \vec{n})$ the Euler flux in the direction of \vec{n} . The unknowns are discontinuous along the cell boundaries and this allows an approximate Riemann solver to be introduced.

The Roe scheme [9] (with low-Mach preconditioning) represents the basic upwind component for the numerical evaluation of the convective fluxes \mathcal{F} :

$$\int_{\partial C_{ij}} \mathcal{F}(W, \vec{n}) d\sigma \simeq \Phi^R(W_i, W_j, \vec{n}) = \frac{\mathcal{F}(W_i, \vec{n}) + \mathcal{F}(W_j, \vec{n})}{2} - \gamma_s d^R(W_i, W_j, \vec{n}) \quad (21)$$

$$d^R(W_i, W_j, \vec{n}) = P^{-1} |P\mathcal{R}(W_i, W_j, \vec{n})| \frac{W_j - W_i}{2} \quad (22)$$

in which W_i is the unknown vector at the i -th node, \vec{n} is the normal to the cell boundary and \mathcal{R} is the Roe Matrix. The matrix $P(W_i, W_j)$ is the Turkel-type preconditioning term, introduced to avoid accuracy problems at low Mach numbers. According to [14], we use this preconditioning only in the stabilizing terms and time consistency is preserved. Finally, the parameter γ_s multiplies the upwind part of the scheme and permits a direct control of the numerical viscosity, leading to a full upwind scheme (the usual Roe scheme) for $\gamma_s = 1$ and to a centered scheme when $\gamma_s = 0$.

The spatial accuracy of quadrature (22) is only first order. Two reconstruction steps are allied for increasing the accuracy. First, the MUSCL linear reconstruction method (“Monotone Upwind Schemes for Conservation Laws”), introduced by Van Leer [16], is adapted. The basic idea is to express the Roe flux as a function of a reconstructed value of W at the boundary between the two cells centered respectively at nodes i and j : $\Phi^R(W_{ij}, W_{ji}, \vec{n}_{ij})$. W_{ij} and W_{ji} are extrapolated from the values of W at the nodes, as follows:

$$W_{ij} = W_i + \frac{1}{2} (\vec{\nabla} W)_{ij} \cdot \vec{i}\vec{j} \quad (23)$$

$$W_{ji} = W_j - \frac{1}{2} (\vec{\nabla} W)_{ji} \cdot \vec{i}\vec{j} \quad (24)$$

Schemes with different properties can be obtained by different numerical evaluation of the slopes $(\vec{\nabla} W)_{ij} \cdot \vec{i}\vec{j}$ and $(\vec{\nabla} W)_{ji} \cdot \vec{i}\vec{j}$. In a second step, the slopes are defined in a parametrized form:

$$\begin{aligned} (\vec{\nabla} W)_{ij} \cdot \vec{i}\vec{j} = & (1 - \beta)(\vec{\nabla} W)_{ij}^C \cdot \vec{i}\vec{j} + \beta(\vec{\nabla} W)_{ij}^U \cdot \vec{i}\vec{j} \\ & + \xi_c \left[(\vec{\nabla} W)_{ij}^U \cdot \vec{i}\vec{j} - 2(\vec{\nabla} W)_{ij}^C \cdot \vec{i}\vec{j} + (\vec{\nabla} W)_{ij}^D \cdot \vec{i}\vec{j} \right] \\ & + \xi_d \left[(\vec{\nabla} W)_M \cdot \vec{i}\vec{j} - 2(\vec{\nabla} W)_i \cdot \vec{i}\vec{j} + (\vec{\nabla} W)_j \cdot \vec{i}\vec{j} \right] \end{aligned} \quad (25)$$

$(\vec{\nabla} W)_{ij}^U$ is the gradient on the upwind tetrahedron T_{ij} , $(\vec{\nabla} W)_{ij}^D$ is the gradient on the downwind tetrahedron T_{ji} , $(\vec{\nabla} W)_i$ is the nodal gradient computed over the finite-volume cell around node i , $(\vec{\nabla} W)_j$ is the nodal gradient computed over the finite-volume cell around node j , $(\vec{\nabla} W)_{ij}^C$ is the centered gradient ($(\vec{\nabla} W)_{ij}^C \cdot \vec{i}\vec{j} = W_j - W_i$) and $(\vec{\nabla} W)_M$ is the gradient at the point M . This last gradient is computed by interpolation of the nodal gradient values at the nodes contained in the face opposite to i in the upwind tetrahedron T_{ij} . The reconstruction of W_{ji} is analogous.

In choosing a particular set of free coefficients (β , ξ_c , ξ_d) in Eq. (25) attention has been dedicated to the dissipative properties of the resulting scheme which is a key point for its successful use in LES simulations. Two schemes have been proposed: the first one (V4) [20] is characterized by $\beta = 1/3$, $\xi_c = \xi_d = 0$, while the latter (V6) [1] is obtained by $\beta = \frac{1}{3}$, $\xi_c = -\frac{1}{30}$ and $\xi_d = -\frac{2}{15}$. The numerical dissipation in the schemes V4 and V6 is made of fourth- and sixth-order space derivatives, respectively, and, thus, it is concentrated on a narrow-band of the highest resolved frequencies. As previously stated, this is important in LES simulations to limit as far as possible the interactions between numerical and SGS dissipation, which could deteriorate the accuracy of the results. The V6 scheme is used in the simulations reported herein.

Time advancing is carried out through an implicit linearized method, based on a second-order accurate backward difference scheme and on a first-order approximation of the Jacobian matrix [27]. The resulting numerical discretization is second-order accurate both in time and space.

4 Numerical results

4.1 Cylinder test-case

Simulations for the flow around a circular cylinder are carried out at Reynolds number based on the cylinder diameter, D , and the freestream velocity, equal to 20000. The computational domain is such that $-10 \leq x/D \leq 25$, $-20 \leq y/D \leq 20$ and $-\pi/2 \leq z/D \leq \pi/2$, where x , y and z denote the streamwise, transverse and spanwise directions respectively, the cylinder center being located at $x = y = 0$. Periodic boundary conditions are applied in the spanwise direction while no-slip conditions are imposed on the cylinder surface. Characteristic based conditions are used at the inflow and outflow as well as on the lateral surfaces. The freestream Mach number is set equal to 0.1 in order to make a sensible comparison with incompressible simulations in the literature. Preconditioning is used to deal with the low Mach number regime. The computational domain is discretized by unstructured grid consisting of approximately 1808485 nodes. Several LES and VMS-LES simulations have been carried by varying SGS models using the dynamic procedure.

Let us start to analyze the results obtained in the simulations carried out around the circular cylinder at Reynold number equal to 20000. For all simulations, statistics are computed by averaging in the spanwise homogeneous direction and in time for 30 vortex shedding cycles. The main bulk flow parameters are summarized in table 1. They are compared with LES results of [6, 18] and the experimental results of [21, 12, 19]. We also report the VMS-LES results of [25] carried out with SGS model of WALE and with the non-dynamic procedure.

For the mean drag coefficient $\overline{C_d}$, experimental values are in the range [1.10 – 1.20]. An overestimation is observed in the LES and in the VMS-LES simulations equipped with the dynamic Smagorinsky model. Conversely, the prediction given by the dynamic VMS-LES approach with the WALE model is better. The obtained value 1.2 well agrees with the experimental data. As for the Strouhal number associated to vortex shedding, St , the value of 0.194 is obtained in the experiments, which well agrees with those obtained in our simulations. Clearly, the mean drag depends on the pressure distribution on the cylinder surface. Figs (1), (2) and (3) show the mean pressure coefficient distribution at the cylinder obtained in the various simulations, together with the experimental data. We can easily see the discrepancy between the numerical results and experimental data obtained by Yokuda (1990), in the dynamic LES simulation and in the dynamic VMS-LES one with the model of Smagorinsky, while the dynamic WALE VMS-LES simulation shows less discrepancy especially at the rear part of the cylinder. For the mean recirculation length, lr , the values obtained by Salvatici et al. in [6] are in the range of [0.7 – 1.4] which well agree with the predictions given with both dynamic LES and VMS-LES simulations. As for the r.m.s of the lift coefficient, the quantitative agreement with the available numerical and experimental data is good for all the considered approaches.

4.2 Sphere test-case

According to the previous analysis, we observe that the variational multiscale LES simulation equipped with the dynamic WALE SGS model provides the best agreement with the experimentals data. Therefore, we adopt this model to compute the flow around a sphere at reynolds numbers equal to 10000 and 50000.

As for the cylinder, the freestream Mach number is set equal to 0.1, and preconditioning is used to deal with the low Mach number regime. We apply the same boundary conditions applied for the cylinder test-case and we use characteristic based conditions at the inflow and outflow as well as on the lateral surfaces.

Next, we continue with the analysis of the simulation carried out around the sphere, first, at Reynolds number equal to 10 000. Table 3 presents the main flow bulk parameters of the VMS-LES simulation equipped with the SGS model of WALE. For the mean drag coefficient, $\overline{C_d} = 0,4$ was obtained in the experiments of Achenbach [7]. This value well agrees with the prediction of our simulation. The mean pressure coefficient distribution over the sphere is shown in Fig 4(a), compared to the reference experimental data of Achenbach [7] at Reynolds number equal to 162000. Furthermore, the agreement in the separation angle is excellent. A value of 82.6 is obtained in our simulation, which totally agrees with the one of 82.5 given by Achenbach [7]. A good agreement is noticed while an overestimation is encountered at $[90^\circ-170^\circ]$.

In the last part of this section, we discuss the behavior of the same model, the VMS-LES with the dynamic SGS model of WALE, used to compute the flow around the sphere at Reynolds number equal to 50000 on the same grid as for $Re=10000$. For the mean recirculation length, the experimental value obtained by Bakic is in the range of $[0.98 - 1.43]$. However, the value given by the dynamic WALE VMS-LES is slightly smaller.

As for the mean drag coefficient, the value of 0.5 obtained in our simulation totally agrees with the experimental values given by Achenbach [7] and Maxworthy [31]. We observe that the separation angle is slightly underestimated when compared to the experimental value of Bakic which is in the range of $[80^\circ-83^\circ]$. The mean pressure coefficient distribution around the sphere at $Re=50000$ is depicted in Fig 4(b). An underestimation is observed by comparison with the experimental result of Bakic. This fact can be explained by the use of a rather coarse grid for the considered Reynolds number.

5 Concluding remarks

A variational multiscale LES approach combined with dynamic SGS models have been presented and used for the simulation of bluff body flows in subcritical regime. More specifically, the simulation of the flow around a cylinder at $Re = 20000$, and the flow around a sphere at $Re = 10000$ and $Re = 50000$ have been carried out. The key ingredients of the used numerics and modeling are : unstructured grids, a second-order accurate numerical scheme stabilized by a tunable numerical diffusion proportional to sixth-order space derivatives, and the VMS-LES approach combined with the dynamic version of Smagorinsky and WALE SGS models. The overall results show the capabilities of the proposed dynamic VMS-LES model to accurately predict the aerodynamic forces acting on the considered bluff bodies, and to properly capture the main flow features associated to such vortex shedding flow problems.

Table 1: Bulk flow parameters predicted by dynamic LES and dynamic VMS-LES around a circular cylinder at Reynolds 20000

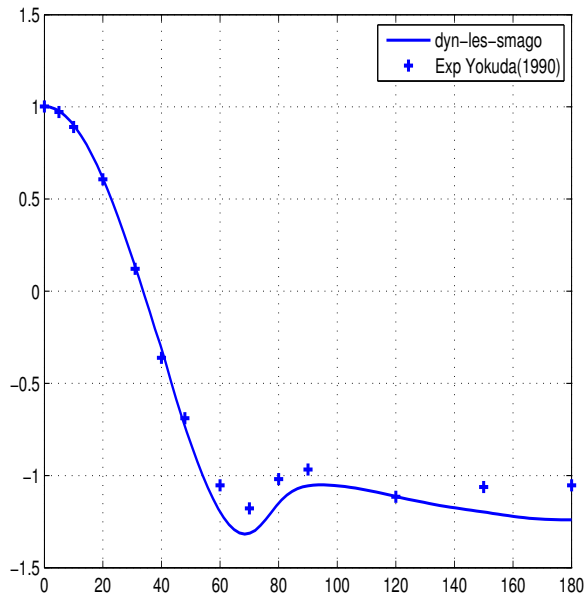
Simulation	$\overline{C_d}$	C_{Lrms}	l_r	$-\overline{C_{pb}}$	θ_{sep}	St
LES Smagorinsky (non-dyn)	1.295	0.574	0.779	1.3	86	.197
LES Smagorinsky dyn	1.24	0.44	0.9	1.24	84	0.19
LES WALE dyn	1.17	0.4	1.182	1.149	84	0.197
VMS-LES Smagorinsky dyn	1.296	0.563	0.852	1.336	86.24	0.186
VMS-LES WALE dyn	1.20	0.44	1.0733	1.197	84	0.191
Experiments [21, 12, 19]	[1.10-1.20]	[0.4-0.6]	–	[1.03-1.09]	–	0.194
LES [6]	[0.94-1.28]	[0.17-0.65]	[0.7-1.4]	[0.83-1.38]	–	–
LES [18]	–	–	1.	[1.04-1.25]	–	–
Vms-LES WALE [25]	1.27	0.60	0.80	1.09	86	0.19

Table 2: Bulk coefficients obtained with the dynamic WALE VMS-LES model for a sphere at Reynolds 50000.

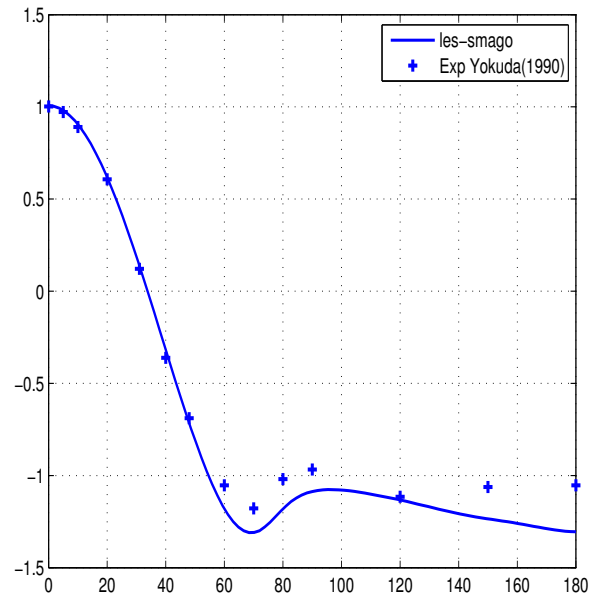
Simulation	$\overline{C_d}$	C_{Lrms}	l_r	$-\overline{C_{pb}}$	θ_{sep}	St
VMS-LES WALE DYN	.50	.05	.83	.32	79	–
VMS-LES-Smagorinsky (S.Wornom)	.44	.04	1.08	.34	85	0.17
Bakic	–	–	.98-1.43	–	80-83	.18
Achenbach(1972),Maxworthy(1969)	.55 , 0.5	–	–	–	–	–

Table 3: Bulk coefficients obtained with the dynamic WALE VMS-LES model for a sphere at Reynolds 10000.

Simulation	$\overline{C_d}$	C_{Lrms}	l_r	$-\overline{C_{pb}}$	θ_{sep}	St
VMS-LES WALE DYN	.43	.02	1.44	.28	82.5	–
Achenbach [7]	.4	–	–	–	82.5	.195



(a)



(b)

Figure 1: Mean pressure coefficient distribution at the cylinder (Reynolds 20000). (a) Simulations with the dynamic LES Smagorinsky model (b) Simulations with the non dynamic LES Smagorinsky model.

References

- [1] S. Camarri, M. V. Salvetti, B. Koobus, and A. Dervieux. A low diffusion MUSCL scheme for LES on unstructured grids. *Comp. Fluids*, 33:1101–1129, 2004.

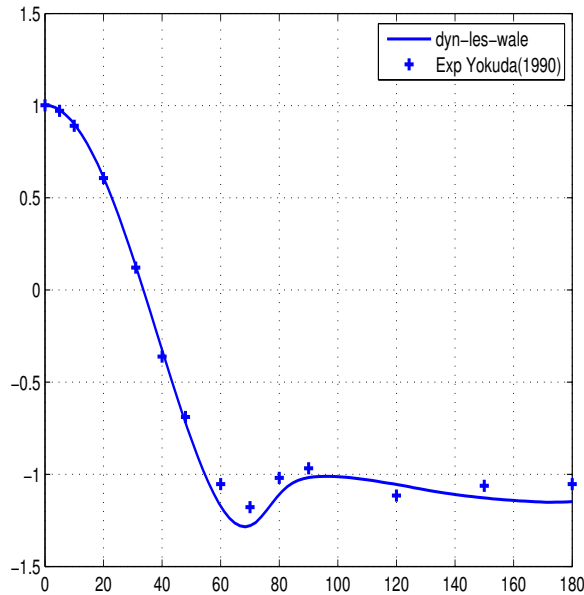


Figure 2: Mean pressure coefficient distribution at the cylinder obtained with the dynamic WALE LES simulation.

- [2] M.H. Lallemand, H. Steve, and A. Dervieux. Unstructured multigridding by volume agglomeration : current status. *Comput. Fluids*, 21 :397-433, 1992.
- [3] C. Farhat, B. Koobus, and H. Tran. Simulation of vortex shedding dominated flows past rigid and flexible structures. In *Computational Methods for Fluid-Structure Interaction*, pages 1–30. Tapir, 1999.
- [4] B. Koobus and C. Farhat. A variational multiscale method for the large eddy simulation of compressible turbulent flows on unstructured meshes-application to vortex shedding. In *Comput. Methods Appl. Mech. Eng.*, 193 :1367-1383, 2004.
- [5] S. Camarri and M. V. Salvetti. Towards the large-eddy simulation of complex engineering flows with unstructured grids. Technical Report RR-3844, INRIA, 1999.
- [6] E. Salvatici and M.V. Salvetti, Large-eddy simulations of the flow around a circular cylinder: effects of grid resolution and subgrid scale modeling, *Wind & Structures*, 6(6):419–436, 2003.
- [7] Achenbach, E.1972 Experiments on the Flow Past Spheres at Very High Reynolds Numbers, *J. Fluid Mech.*, 54(3),pp. 565-575.
- [8] H. Ouvrard, B. Koobus, A. Dervieux, and M.V. Salvetti. Classical and variational multiscale LES of the flow around a circular cylinder on unstructured grids. *Comp. Fluids*, 2010;39:1083-94.
- [9] P.L. Roe. Approximate Riemann solvers, parameters, vectors and difference schemes. In *J. Comp. Phys.*, 43 :357-371, 1981.
- [10] H. Baya Toda, Karine Truffin and Franck Nicoud, Is the dynamic procedure appropriate for all SGS model, *V European Conference on Computational Fluid Dynamics, ACCOMADS CFD 2010*, Lisbon, Portugal, 2010.
- [11] J. Blazek. Computational Fluid Dynamics: Principles and Applications. In *Elsevier Science Ltd*, Oxford England, 2001.

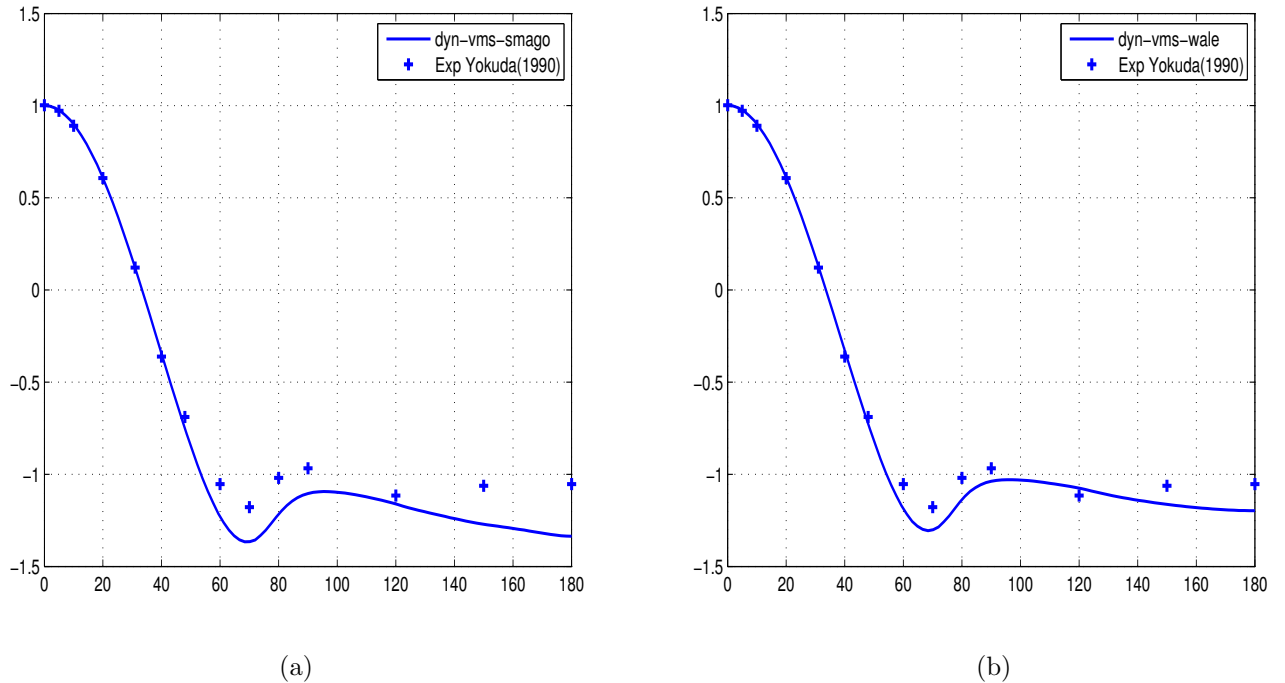


Figure 3: Mean pressure coefficient distribution at the cylinder (Reynolds 20000). (a) VMS-LES simulations with the dynamic SGS model of Smagorinsky. (b) VMS-LES simulations with the dynamic SGS model of WALE.

- [12] R.I. Basu, Aerodynamic forces on structures of circular cross-section. part i: Model-scale data obtained under two-dimensional and low-turbulence streams, *J. Wind Eng. Ind. Aerodynamic*, 21:273–294, 1985.
- [13] V. Bakic, Experimental investigation of a flow around sphere, ,1, 63-81 2004.
- [14] H.Guillard and C. Viozat. On the behaviour of upwind schemes in the low Mach number limit. *Computers and Fluids*, 28 :63-86, 1999.
- [15] J. Frohlich and W. Rodi. Introduction to large eddy-simulation of turbulent flow. In *Institute of Hydromechanics*, University of Karlsruhe, Germany, p. 1-19.
- [16] B. Van. Leer. Towards the ultimate conservative scheme. IV :A new approach to numerical convection. In *J. Comp. Phys.*, 23 :276-299, 1977.
- [17] V. Bakic and M. Peric Visualization of flow around sphere for reynolds numbers between 22 000 and 400 000, *Thermophysics and Aeromechanics*, 2005, Vol.12, No. 3.
- [18] S. Aradag Unsteady turbulent vortex structure downstream of a three dimensional cylinder *J. of Thermal Science and Technology* 29:1, 91-98, 2009
- [19] S. Yokuda and R.R. Ramaprian, The dynamics of flow around a cylinder at subcritical reynolds number, *Phys. Fluids A*, 5:3186–3196, 1990.
- [20] S. Camarri, M.V. Salvetti, B. Koobus, and A. Dervieux. Large-eddy simulation of a bluff-body flow on unstructured grids. *Int. J. Num. Meth. Fluids*, 40:1431–1460, 2002.
- [21] C. Norberg, Fluctuating lift on a circular cylinder: review and new measurements, *J. Fluids Struct.*, 17: 57–96, 2003.
- [22] T.J.R. Hughes, L.Mazzei, and K.E. Jansen. Large-eddy simulation and the variational multiscale method. *Comput. Vis. Sci.*,3 :47-59,2000.

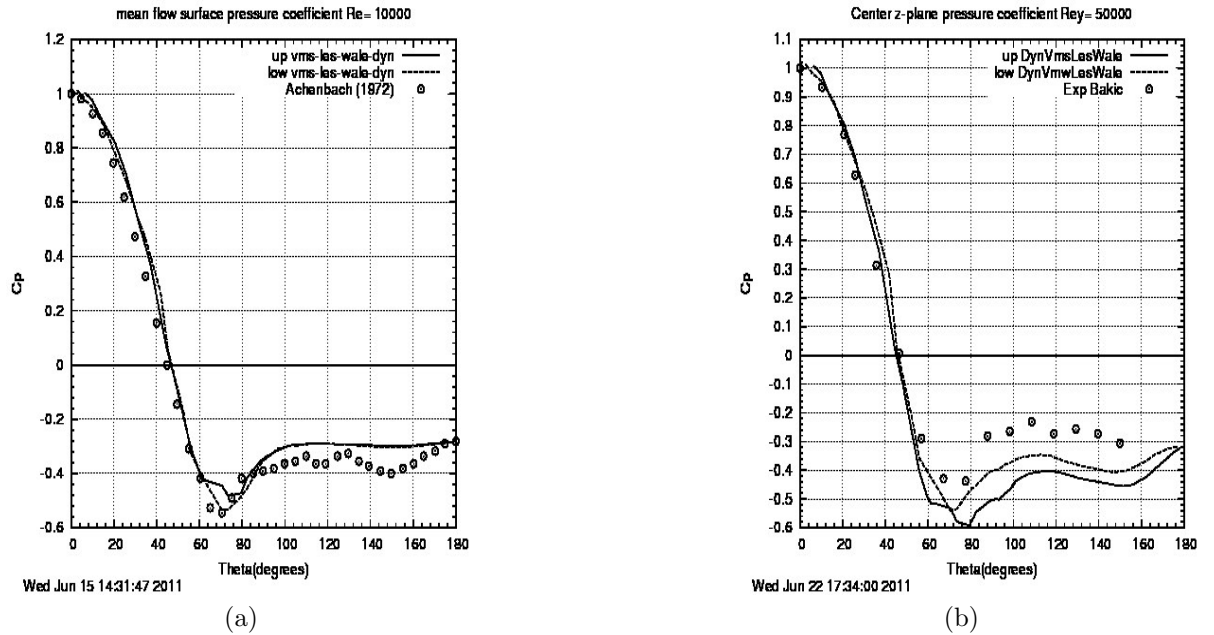


Figure 4: Mean pressure coefficient distribution at the sphere obtained with the dynamic WALE VMS-LES model. (a) Reynolds=10000. (b) Reynolds=50000.

- [23] T.J.R. Hughes and A.A. Oberai and L. Mazzei. Large eddy simulation of turbulent channel flows by the variational multiscale method. *Phys. Fluids*, 13 :1784–1799, 2001.
- [24] J. Smagorinsky. General circulation experiments with the primitive equations. *Month. Weath. Rev.*, 91(3) :99-164, 1963.
- [25] Wornom S et al. Variational multiscale large-eddy simulations of the flow past a circular cylinder: Reynolds number effects. *Comput Fluids (2011)*, doi:10.1016/j.compfluid.2011.02.011.
- [26] F. Nicoud and F. Ducros. Subgrid-scale stress modelling based on the square of the velocity gradient tensor. *Flow Turb. Comb.*, 62(3) :183-200, 1999.
- [27] R. Martin and H.Guillard . A second-order defect correction scheme for unsteady problems. *Comput. and Fluids*, 25(1) :9-27, 1996.
- [28] M. Germano, U. Piomelli, P. Moin, W.H. Cabot, A Dynamic Subgrid-Scale Eddy Viscosity Model, *Physics of Fluids*, A 3, 1760-1765, 1991.
- [29] D. K. Lilly, A proposed modification of the Germano subgrid scale closure model, *Physics of Fluids*, A 4, 633, 1992.
- [30] S. Ghosal, T. Lund, P. Moin, K. Akselvoll, The dynamic localization model for large eddy simulation of turbulent flows, *J. Fluid Mech.*, 286, 229-255.
- [31] T. Maxworthy, Experiments on the flow around a sphere at high. Reynolds numbers, *J. Appl. Mech.*, E36, 598, 1969.